Preamble Signal Shortening Methods Employing Channel Bonding in MIMO-OFDM Base Wireless LAN Systems

MUGURO, J. K.* and KUBOTA, S.
Graduate school of Science and Engineering, Shibaura Institute of Technology, 3-7-5 Toyosu, Koto, Tokyo, 135-8548, Japan
E-mail: muguro.joseph@gmail.com, kubota@sic.shibaura-it.ac.jp

Abstract
MIMO-OFDM is the generally accepted standard in the recent WLAN systems. However, this method increases training signals required to estimate the propagation matrix of multi-antenna system employed by IEEE 802.11ac and above. In this study, we investigate methods of shortening Very High Throughput-Long Training Field (VHT-LTF) preamble signal in WLAN systems to improve the effective throughput performance of the system. On the transmitter side, preamble shortening routine is employed and a subsequent recovery on the receiver side using estimation algorithms. Several data recovery methods were evaluated with different reduction schemes of the preamble signal. Simulation results have shown that ½ VHT-LTF Preamble can be used while maintaining a considerable transmission performance.
Keywords: IEEE 802.11, MIMO-OFDM, WLANs, pilot channel estimation,

1. INTRODUCTION

In the recent past, mobile data traffic has been on the increase due to an increase in data-intensive communication services like HD Video streaming, Voice over Wi-Fi, as well as sophisticated devices like smart-phones, personal computers, digital wearables amongst others. Estimates for Global IP data traffic is expected to surpass the zettabyte (10^{27}) threshold by 2016 (CiscoReport, 2016). Mobile traffic for the year 2015 was approximately 44 Exabyte up from 30 Exabyte the previous year. There are two key features in mobile communication systems; mobility and data rate (Nee & Prasad, 2000). An increase in mobility results in significant reduction in data rate as witnessed in mobile broadband systems like 3G. Technological advancements are bridging the gap between mobility and data rate by introducing localized, semi-temporal wireless communications in this case WLANs. From a report (CiscoReport, 2016), up to 46 percent of the mobile data traffic is offloaded to WLAN systems. This and other reasons have led to a steady increase popularity of WLAN systems.

The IEEE 802.11a/b/g/n/ac WLANs have been successfully deployed with each subsequent standard addressing a different optimization feature of the network. The most recent update, IEEE 802.11ac, increased the communication antennas from four to eight, extended the operational bandwidth from 20/40 MHz to 160MHz, as well as other optimization schemes to cater for increasing data rate requirement (Khan, Gonzalez, & Park, 2016). The high data rate requirements for the next-generation WLAN pose a challenge for physical layer (PHY) implementation technologies. With this challenge at hand, a lot of research work has been carried out to enhance the throughput of next-generation WLAN system.

Multiple Input Multiple Output-Orthogonal Frequency Division Multiplexing (MIMO -OFDM) system is the standardized communication system for the recent releases of WLANs (IEEEp802.11, 2013). MIMO-OFDM system address the data rate challenge in two major approaches; the use of smart antennas as a spatial division multiplexing (SDM) strategy and OFDM as a robust air-interface strategy (Nee & Prasad, 2000). The principle of OFDM is splitting the high-rate data streams in to subsequent low rate streams in frequency domain and transmitting them simultaneously through multiple subcarriers. This results in an increase in the symbol duration for the lower rate parallel subcarriers. Consequently, the relative amount of dispersion caused by multipath delay spread during transmission is decreased. A guard interval is introduced for every OFDM symbol to mitigate inter-symbol interference. The OFDM symbol is also appended with a cyclic extension to avoid inter-carrier interference. MIMO system as a key feature in communication focuses on transmitting different data streams (spatial streams) on multiple antennas. When spatial streams are used with MIMO this is termed as SDM. The data rate of SDM/MIMO system increases as a function of independent data streams. As with any communication model in place, WLANs' coherent detection of the transmitted data is a significant issue. The main issue in detection is how to find the reference values without introducing too many training overhead. Channel estimation in packet based transmission is simpler because the packet duration is short enough to assume a constant channel during packet transmission length. In spite of this, training pilots inserted over several scattered OFDM data symbols introduces a delay of several symbols before the channel estimate can be acquired. Such symbol delay is highly undesirable particularly in packet transmission which require a successful transmission acknowledgement (ACK) as prescribed in carrier sense multiple access with Collison avoidance (CSMA-CA). To address this issue, packet transmission utilizes preamble/training signal consisting of one or more known OFDM symbol in the beginning of the transmission followed by pilot signal to track the changes as they occur in the channel.

WLANs include various training fields in the transmission symbols as described above. As expected, with the recent update to 8 MIMO system, the training field overhead is a big problem which this research tries to solve. The Very High Throughput-Long Training Field (VHT-LTF) provides a means for receivers to estimate MIMO channels in WLAN systems. How to design VHT-LTF sequences for next-generation WLAN systems is a tough task. Excellent VHT-LTFs should both minimize the channel estimation errors and reduce the preamble overhead as much as possible (Zhang, Wang, & Kang, 2011).

Previous research focused on channel estimation methods and analysis improvement. An example is (Hoefel, Nov. 2014) that seek to improve sphere decoding and successive Interference cancellation (SIC) for IEEE 802.11ac. A paper focusing on channel estimation in frequency domain as a simplification of the estimation matrix is reported in (Al-Naffouri, Islam, Al-Dhahir, & Lu, April 2010). One paper (Zhang, Wang, & Kang, 2011), attempted to address the problem of LTF by proposing optimal pilot field in place of the current 8 LTF fields. This approach looks overly ambitious as well as computational complexities while in system integration. A previous research is reported here (Takahashi & Kubota, 2014) which this research builds on.

The rest of this paper is organized as follows, Section II is the System design for IEEE 802.11 WLAN, Section III is the proposed Training signal design with special focus on VHTLTF signal, Section IV outlines the simulations and the obtained results, section V is the conclusion of the paper.

2. SYSTEM MODEL

WLANs Transmitter communication block diagram is as shown in figure 1 below. The scrambler arranges the input data to reduce the probability of long sequences of 0s or 1s while the encoder parser demultiplexes the scrambled bits in a round robin manner. Forward Error Correction (FEC) encoders are employed in the system to enable error correction on the receiver side. Stream parser divides the data into blocks for interleaving (changing the order of bits to prevent bust errors) and constellation mapping (mapping the sequence of bits in each stream to constellation points). Interleaving is applied only when BCC encoding is used (Perahia & Stacey., 2013).

STBC encoder spreads constellation points from spatial streams into space-time streams using a space-time block code. This is used only when Nss<Nsts (where Nss is the Number of spatial streams and Nsts is the Number of transmission antennas). Inverse discrete Fourier transform (IDFT) is employed which converts a block of constellation points to a time domain block while the GI insertion block prepends to the symbol a circular extension of itself. Windowing optionally smooths the edges of each symbol to ensure a more compact spectrum.

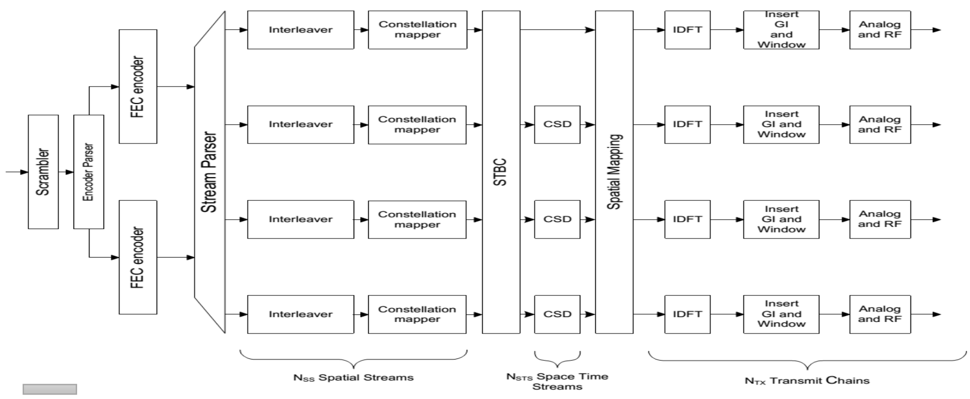

Fig. 1: Transmitter block diagram

2.1 Preamble signal design

From the standardization of IEEE 802.11, the Physical layer convergence procedure (PLCP) sublayer provides a convergence procedure for converting PLCP service data units (PSDUs) to or converted from PLCP protocol data units (PPDUs). During transmission, the PSDU is provided with a PLCP preamble and header to create the PPDU. At the receiver, the PLCP preamble and header are processed to facilitate demodulation and recovery of the PSDU (IEEEp802.11, 2013). As mentioned above, the 802.11 standard uses the training preambles to recover the transmitted data. The packet structure of 802.11ac is as shown in figure 2 below. The legacy fields (L-LTF, L-STF and L-SIG) are used to maintain backward compatibility with other releases in the network. More details can be obtained in detailed WLAN book (Perahia & Stacey., 2013).

The VHT-STF is used for time synchronization as well as automatic gain control estimation. VHT-LTF is used for frequency offset as well as channel estimation. A VHT-LTF field is transmitted for each spatial stream as indicated by the MCS. For a 40MHz transmission, the VHT-LTF sequence is as shown in the figure 3. The mapping matrix is defined as follows

$$\mathbf{P}_{\mathrm{VHTLTF},4\mathrm{x}4} = \begin{bmatrix} 1 & -1 & 1 & 1 \\ 1 & 1 & -1 & 1 \\ 1 & 1 & 1 & -1 \\ -1 & 1 & 1 & 1 \end{bmatrix} \quad (1)$$

For an 8 spatial streams, the P matrix is defined by the equation (2) below.

$$\mathbf{P}_{\mathrm{VHTLTF},8\mathrm{x}8} = \begin{bmatrix} \mathbf{P}_{\mathrm{VHTLTF},4\mathrm{x}4} & \mathbf{P}_{\mathrm{VHTLTF},4\mathrm{x}4} \\ \mathbf{P}_{\mathrm{VHTLTF},4\mathrm{x}4} & -\mathbf{P}_{\mathrm{VHTLTF},4\mathrm{x}4} \end{bmatrix} \quad (2)$$

The orthogonal mapping matrix is multiplied with the sequence to generate the training field.

The VHT-SIG conveys information about transmission parameters. VHT-SIG-A carries parameters like Bandwidth in use, STBC usage, number of spatial streams etc. VHT-SIG-B contains parameters like size of GI, MCS in use, CRC in use amongst others (IEEEp802.11, 2013). In the paper, we will focus on the study of LTF. The data field is formed by the data units to be transmitted after encoding processes described earlier. Tail and padding is included to complete the packet structure.

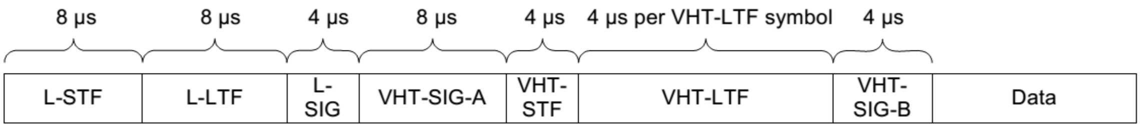

Field	Description
L-STF	Non-HT Short Training field
L-LTF	Non-HT Long Training field
L-SIG	Non-HT SIGNAL field
VHT-SIG-A	VHT Signal A field
VHT-STF	VHT Short Training field
VHT-LTF	VHT Long Training field
VHT-SIG-B	VHT Signal B field
Data	The Data field carries the PSDU(s)

Fig. 2: IEEE 802.11 packet structure and timing related constants

$$LTF_{\mathrm{left}} = \{1, 1, -1, -1, 1, 1, -1, 1, -1, 1, 1, 1, 1, 1, 1, -1, -1, 1, 1, -1, 1, -1, 1, 1, 1, 1\}$$

$$LTF_{\mathrm{right}} = \{1, -1, -1, 1, 1, -1, 1, -1, 1, -1, -1, -1, -1, -1, 1, 1, -1, -1, 1, -1, 1, -1, 1, 1, 1, 1\}$$

$$\begin{aligned} VHTLTF_{-28,28} &= \{1, 1, LTF_{\mathrm{left}}, 0, LTF_{\mathrm{right}}, -1, -1\} \\ &= HTLTF_{-28,28} \end{aligned}$$

$$\begin{aligned} VHTLTF_{-58,58} &= \{LTF_{\mathrm{left}}, 1, LTF_{\mathrm{right}}, -1, -1, -1, 1, 0, 0, 0, -1, 1, 1, -1, LTF_{\mathrm{left}}, 1, LTF_{\mathrm{right}}\} \\ &= HTLTF_{-58,58} \end{aligned}$$

Fig. 3: VHT-LTF sequence generator matrix for 20 / 40MHz.

2.2 Extended bandwidth allocation

The 11ac device is required to support 20, 40, 80 and an optional 160MHz channel bandwidth. The 80MHz channel will consist of two adjacent, non-overlapping 40MHz channels. The 160MHz channel is formed by two 80MHz channels which may be adjacent (contiguous) or non-contiguous as shown in fig. 4 below. This channel configuration is referred to as channel bonding.

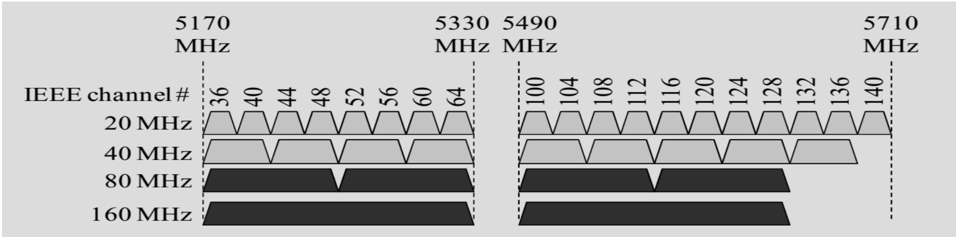

Fig. 4: Europe and Japan Bandwidth and channel allocation.

3. PROPOSED METHODS

The proposed system is designed to reduce the number of required VHT-LTF fields. The mapping matrix was changed to produce a VHT-LTF signal as shown in the figure 5 below while maintaining the orthogonality. On the receiver side, various data fitting techniques are employed to recover the omitted data. Spline interpolation method and RBFN method have been evaluated and reported in this paper. The methods proposed are briefly described below.

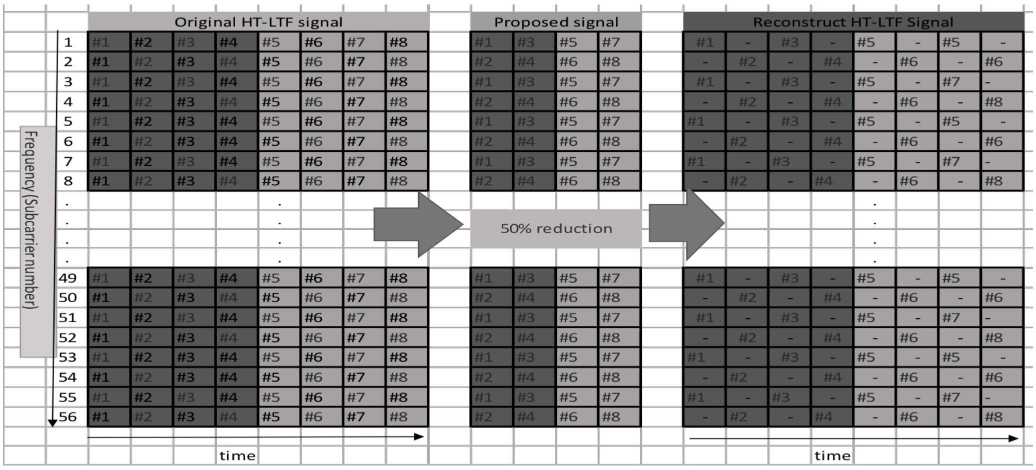

Fig. 5: Proposed system with ½ VHT-LTF preamble

3.1 RBFN Method

A Radial Basis Function Network (RBFN) is a particular type of neural network. The RBF network model is motivated by the locally tuned response observed in biologic neurons. Neurons with locally tuned characteristics are present in several parts of the neural system like the auditory system and color selectivity of visual system (Schwenker, Kestler, & Palm., 2001). The neurons responds to a small range of the input space to achieve the holistic neural response characteristic.

The RBF Network is mostly applied in solutions to exact interpolation problems. RBF mapping passes through every data point (x^u, y^u). RBFN as applied in neural network consists of three neural layers as shown in figure 6; a layer of input neurons feeding the feature vectors into the network, a hidden layer of RBF neurons which calculate the outcome of the basis functions and a layer of output neurons, calculating a linear combination of the basis functions

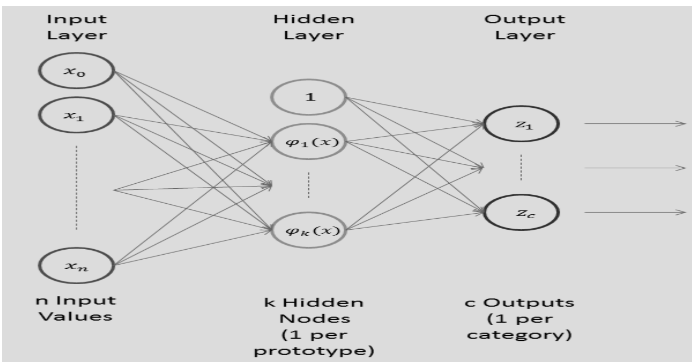

Fig. 6: Typical architecture of an RBF Network.

3.1.1 Training the RBFN

The training process for an RBFN consists of selecting three sets of parameters: the prototypes (mu) and beta coefficient for each of the RBF neurons, and the matrix of output weights between the RBF neurons and the output nodes. A major advantage in RBFN is the ease of training the network; it's possible to determine suitable function parameters without a full non-linear optimization of the whole network (Schwenker, Kestler, & Palm., 2001). For a given input pattern $x \in$ s, the typical output of an RBFNN function o(x) is given as;

$$o(x) = \sum_{i=1}^{N} w_i \varphi(\|x - \mu_i\|) \quad (3)$$

Where N is the number of neurons in the hidden layer, w_i is the weight and μ_i is the center point of the i-th neuron.

The function $\varphi(x, \mu_i)$ is the radial function and is generally taken as the Gaussian of the form

$$\varphi(\|x - \mu_i\|) = e^{-\beta\|x-\mu_i\|^2} \quad (4)$$

Where **β** is a parameter that controls the kernel width.

Several approaches for parameter selection exist in literature, fixed centers, and cluster-based approach amongst others (Bishop, 2007). This paper focuses on k-Means clustering approach due to the issues present in fixed centers namely, the data points may not be evenly distributed in the input space. In clustered approach, the aim is to determine a small but representative set of centres or prototypes from a larger data set in order to minimize some quantization error. This approaches identify subsets of neighboring data points and use them to partition the input space, and then an RBF center can be placed at the center of each cluster. Once the RBF centres have been determined in this way, the RBF width is then set according to the variances of the points in the corresponding cluster.

The K-Means clustering algorithm as described in (Bishop, 2007) picks the number K of centres and randomly assigns the data points $\{x^p\}$ to K subsets. It then uses a simple re-estimation procedure to end up with a partition of the data points into K disjoint sub-sets or clusters S_j containing N_j data points that minimizes the sum squared clustering function

$$J = \sum_{j=1}^{K} \sum_{p \in S_j} \|\mathbf{x}^p - \boldsymbol{\mu}_j\|^2 \quad (5)$$

Where μ_j is the mean/centroid of the data points in the set. The algorithm finds the nearest mean μ_j of each data point x^p and reassigns the data to the associate cluster Sj and then recomputes the mean μ_j as given by (6) below.

$$\boldsymbol{\mu}_j = \frac{1}{N_j} \sum_{p \in S_j} \mathbf{x}^p \quad (6)$$

The clustering process terminates when no more data points switch from one cluster to another.

3.1.2 Calculating the kernel widths

The setting of the kernel widths is a critical issue in the transition to the RBF network (Bishop, 2007). When the kernel width β is too large, the estimated probability density is over-smoothed and the nature of the underlying true density may be lost. Conversely, when it is too small there may be an over-adaptation to the particular data set.

3.2 Spline Method

A spline function consists of polynomial pieces on subintervals joined together with certain continuity conditions. A spline of degree 3 is a cubic spline, degree 2 is a quadratic spline, degree 1 is a linear function while a degree 0 is a piecewise constants. Si in the equation below is a third degree polynomial that we wish to consider piecewise to arrive at a cubic spline.

$$S_i(x) = a_i(x - x_i)^3 + b_i(x - x_i)^2 + c_i(x - x_i) + d_i \quad (7)$$

For i = 1, 2, …., n−1.

From the polynomial equation above, we consider n points, $x_1, x_2, x_3, \ldots, x_n$ which satisfy $x_1<x_2<x_3 <x_n$. These points are referred to as knots by which we evaluate the spline function. A spline function of degree k having knots $x_1, x_2, x_3, \ldots, x_n$ is a function S such that;

a. On each interval $[x_{i-1}, x_i]$, S is a polynomial of degree ≤ k.

b. S has a continuous k^{st} derivative on $[x_1, x_n]$.

The requisite idea of a spline is to avail a means of connecting any two adjacent data points using an equation or to fit piecewise function of the form (Daud, Yahya, Nayan, Sagayan, & Talib, 2011).

$$S(x) = \begin{cases} S_1(x) & x \in [x_1, x_2] \\ S_2(x) & x \in [x_2, x_3] \\ & \\ S_{n-1}(x) & x \in [x_{n-1}, x_n] \end{cases} \tag{8}$$

Where S(x) is as defined in equation 7 above. The following are the conditions necessary to ensure that the interpolation in Cubic spline works (Daud, Yahya, Nayan, Sagayan, & Talib, 2011).

1. The piecewise function S (x) will interpolate all data points on the interval $[x_1, x_n]$.
2. S(x) will be continuous on the interval $[x_1, x_n]$.
3. S'(x) will be continuous on the interval $[x_1, x_n]$.
4. S''(x) be continuous on the interval $[x_1, x_n]$.

A major advantage of Spline interpolation is that it has the ability to correlate data which doesn't follow specific pattern without a single polynomial's extreme behavior (Daud, Yahya, Nayan, Sagayan, & Talib, 2011). According to (Unser, 2003) splines provide a unique platform for establishment of a link between the continuous and discrete domains. This makes cubic spline technique one of the very best data fitting approach. This is part of the reason why this paper considered cubic spline for the data fitting of the recovered signal.

4. SIMULATION RESULTS

We modelled PHY layer of IEEE 802.11ac WLAN system in Matlab simulations to verify the results of the research. The parameters used for the simulation are listed in the table below.

Table 1. Simulation parameters

IEEE802.11ac Parameters	Values
Modulation order (M)	OFDM (QPSK, 16QAM, 64QAM, 256QAM)
Coding rate (Rc)	1/2, 2/3 3/4, 5/6
No of Spatial Streams (Nss)	8
Sub-Carrier number	114（Pilot:6 Data:108）
FFT size	128
OFDM symbol size	4.0u sec (Guard Interval: 0.8 u sec)
Bandwidth	40 MHz
Channel Model	TGn B (Home environment) TGn C (Small office environment)
Doppler frequency size	3 Hz
Payload size	1,500 Byte

The following results were obtained using 40MHz bandwidth allocation.

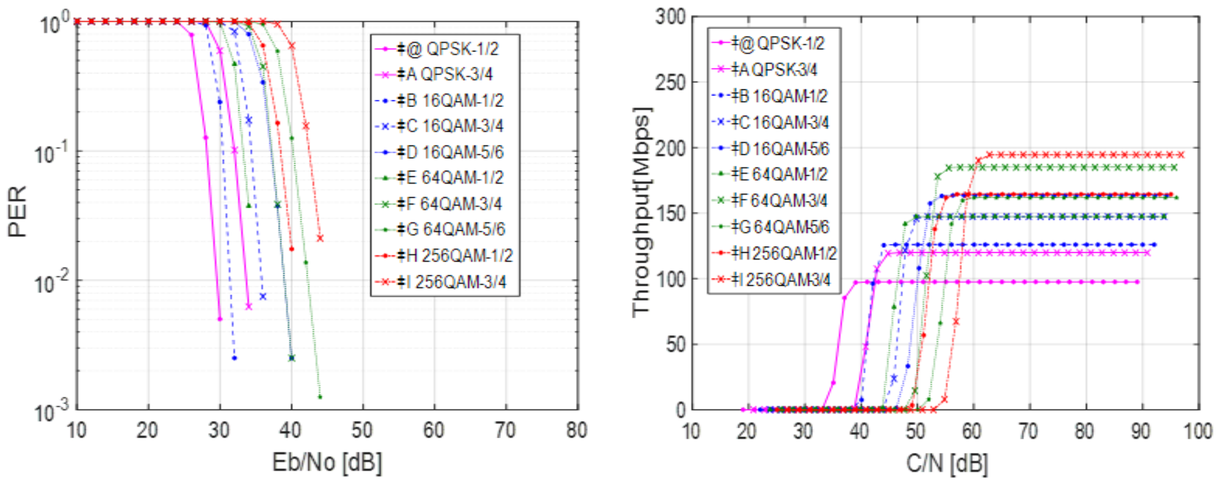

Fig. 7: PER and Effective Throughput performance of conventional 802.11ac TGn B

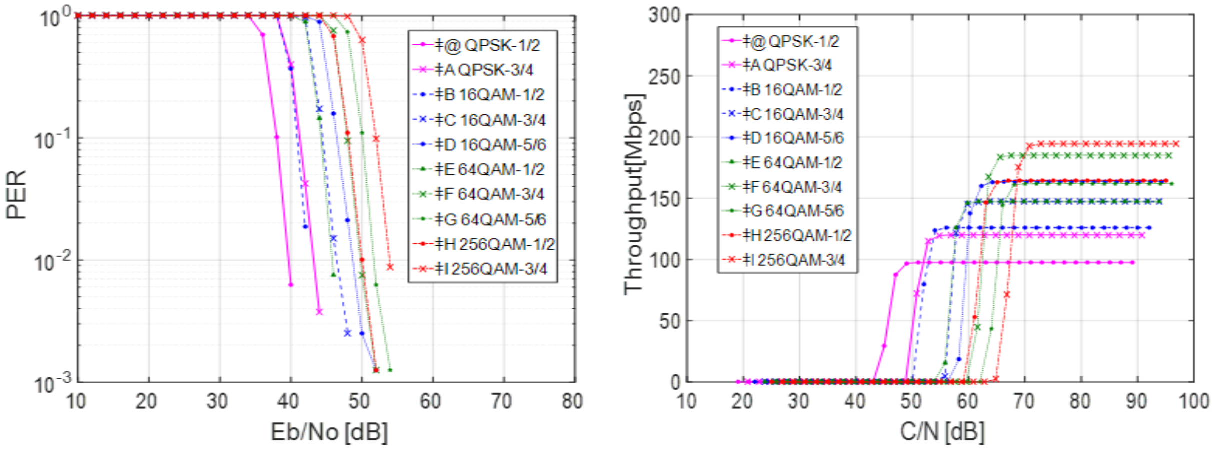

Fig. 8: PER and Effective Throughput performance of conventional 802.11ac TGn C

From the figures 7 and 8, the conventional effective maximum throughput possible for an 8x8 MIMO is approximately 200 Mbps. The PER performance range is 30 to 50 of Eb/No for a 10^{-2} error rate for the entire modulation schemes in TGn B environment. In the case of TGn C as shown in figure 8, the range is 40 to 60 of Eb/No.

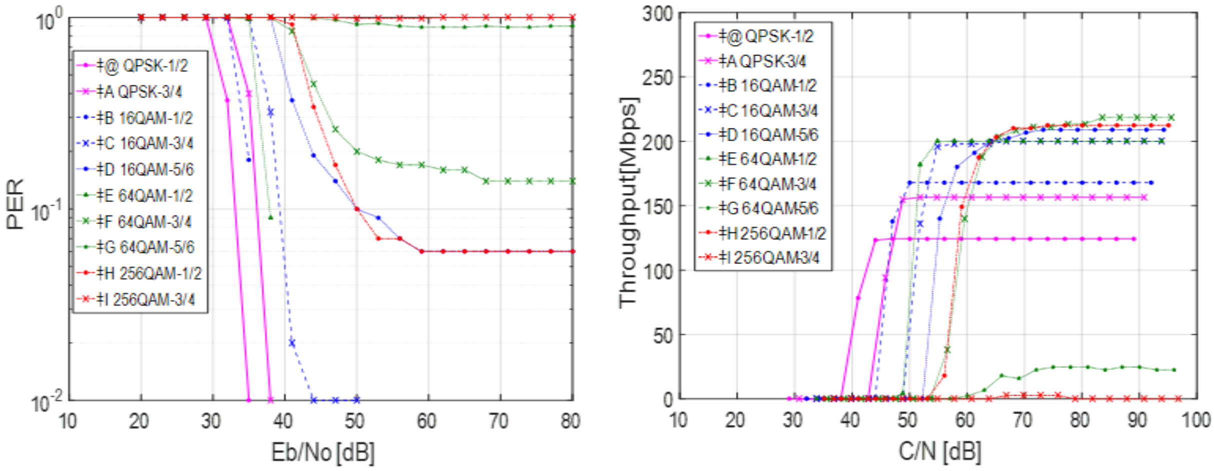

Fig. 9: PER and Effective throughput performance of ½ VHT-LTF preamble using RBFN method TGn B

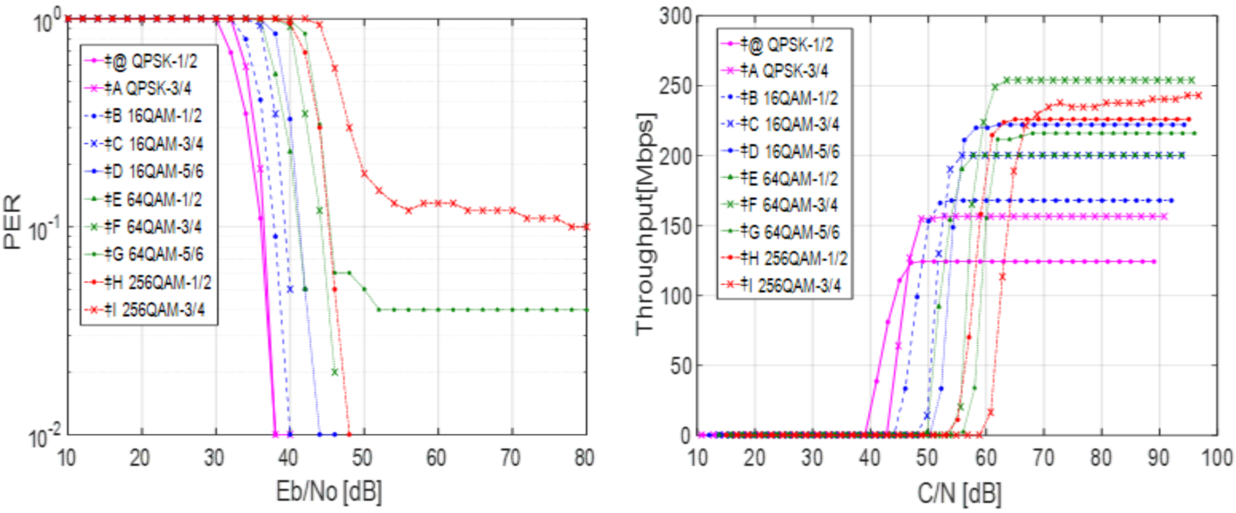

Fig. 10: PER and Effective Throughput performance of ½ VHT-LTF preamble using Spline method TGn C

For figure 10, the PER is similar to that TGn C conventional method apart from higher order modulation schemes which have an error floor. In spite of this, the throughput performance improves several folds from the conventional as shown by the table below. In RBFN method as seen in figure 9, higher order modulation schemes performs poorly but the lower schemes surpasses the conventional method. The overall throughput performance is as captured below at C/N of 70dB.

Table 2: Effective throughput performance in Mbps.

Modulation scheme	FEC rate	Conventional TGn B	RBFN TGn B	Throughput Improvement TGn B	Conventional TGn C	Spline TGn C	Throughput Improvement TGn C
QPSK	1/2	98	125	27	98	125	27
	3/4	120	157	37	120	157	37
16 QAM	1/2	126	168	42	126	168	42
	3/4	148	200	52	148	200	52
	5/6	164	206	42	164	222	58
64 QAM	1/2	148	200	52	148	200	52
	3/4	185	210	25	185	254	69
	5/6	162	20	0	162	216	54
256 QAM	1/2	165	210	45	165	226	61
	3/4	195	3	0	195	235	40

The throughput improvement shown above is quite significant in addressing the high data rate challenge. The table shows an average improvement of about 22% and 32% for RBFN and Spline method respectively as compared to the conventional method with preamble shortening effect.

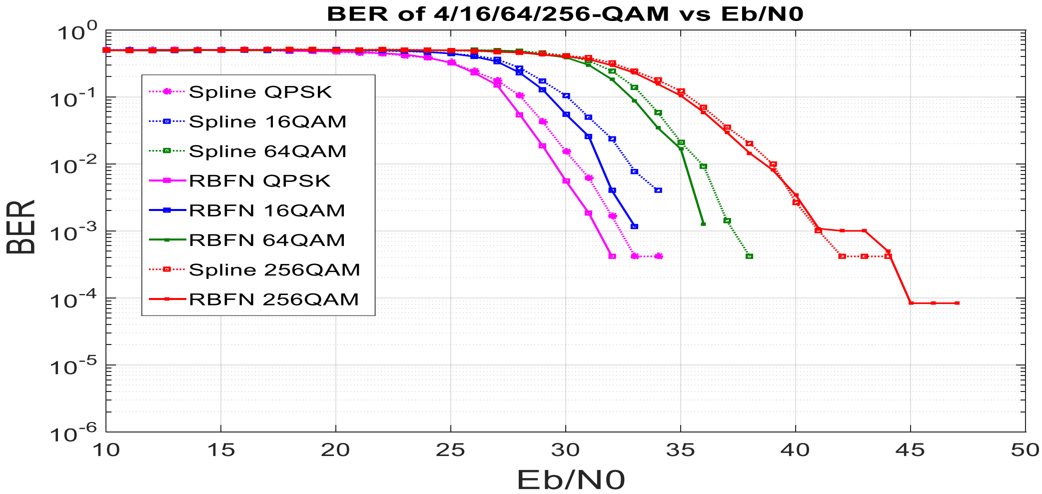

Fig. 11: BER Comparison of spline and RBFN method

The figure 11 shows comparison of the two methods in use for different QAM modulation schemes. Comparatively, RBFN method performs better than Spline method for lower order modulation schemes. However, the spline out performs the RBFN for higher order modulation schemes. This can be attributed to the robustness of the spline method to correlate drastic changes in the received data with higher modulations.

5 CONCLUSION

From the above results, we established that transmission of data with ½ VHT-LTF preamble is possible. Besides, the preamble reduction schemes leads to significant throughput improvement using easy implementation methodologies. This may be attributed to the extra time generated for useful data transmission totaling up to 16 u sec for VHT-LTF of 4 symbols. From the results, a combination approach for the two methods can be adopted to give optimal BER performance in the low and high order modulation schemes.

Reference

Al-Naffouri, T., Islam, K., Al-Dhahir, N., & Lu, S. (April 2010). A Model Reduction Approach for OFDM Channel Estimation Under High Mobility Conditions. *Signal Processing, IEEE Transactions on , vol.58, no.4, pp.2181-2193.*

Bishop, C. M. (2007). *Pattern Recognition and Machine Learning. .* New York: Springer.

CiscoReport. (2016). *Cisco VNI:Forecast and Methodology, 2015–2020.* cisco. Retrieved August 15, 2016, from http://www.cisco.com/c/dam/en/us/solutions/collateral/service-provider/visual-networking-index-vni/complete-white-paper-c11-481360.pdf

Daud, H., Yahya, N., Nayan, M. Y., Sagayan, V., & Talib, M. (2011). A scaled experiment for verificaton of SPLINE interpolation technique. *Industrial Electronics and Applications (ISIEA), 2011 IEEE Symposium* , (pp. 320-3). Langkawi .

Hoefel, R. (Nov. 2014). IEEE 802.11ac WLANs: A performance evaluation of sphere decoding and lattice reduction MMSE-SIC MIMO detectors. *2014 IEEE Latin-America Conference (LATINCOM) vol., no., pp.1-6, 5-7* .

IEEEp802.11. (December 2013). *IEEE Standard for Wireless LAN Medium Access Control (MAC) and Physical Layer (PHY) Specifications, Amendment 4: Enhancement for Very High Throughput for Operations in Bands below 6 GHz.* IEEE P802.11ac,.

Khan, G. Z., Gonzalez, R., & Park, E. C. (2016). A performance analysis of MAC and PHY layers in IEEE 802.11ac wireless network," , , pp. *18th International Conference on Advanced Communication Technology (ICACT), Pyeongchang Kwangwoon Do, South Korea*, (pp. 20-).

Nee, R., & Prasad, R. (2000). *OFDM wireless multimedia communications. .* Boston: Artech House.

Perahia, E., & Stacey., R. (2013). *Next Generation Wireless Lans: 802.11n and 802.11ac.* Cambridge: Cambridge University Press.

Schwenker, F., Kestler, H., & Palm., G. (2001). Three Learning Phases for Radial-Basis-Function Networks. *Neural Networks : the Official Journal of the International Neural Network Society.* (14), 4-5.

Takahashi, T., & Kubota, S. (2014). A Study of Training Signal Shortening Method in MIMO-OFDM Base Wireless LAN Systems. *IEICE Technical report of Short Range Wireless comm, SRW2014-39, vol., 114, no. 367, pp. 23-28, 2014-12. 114.* Tokyo: Unpublished.

Unser, M. (2003). Splines and Wavelets: New Perspectives for Pattern Recognition. *25th DAGM Symposium*, (pp. 244-248). Magdeburg, Germany.

Zhang, W., Wang, J., & Kang, G. (2011). A novel High Throughput Long Training Field sequence design for next-generation WLAN. *Wireless Telecommunications Symposium (WTS) 2011*, (pp. pp. 1-5.). New York City, NY.